Energy & Environmental Science

Cite this: *Energy Environ. Sci.*, 2011, **4**, 1522

www.rsc.org/ees

PAPER

Palladium thorn clusters as catalysts for electrooxidation of formic acid

Hui Meng,*[a] Chengxin Wang,[a] Pei Kang Shen*[a] and Gang Wu[b]

Received 23rd November 2010, Accepted 15th February 2011
DOI: 10.1039/c0ee00702a

Pure palladium thorn clusters were synthesized using the electrodeposition method. The clusters were composed of several thorns growing on one basis. Each thorn was composed of hexahedral units with decreasing sizes. The whole thorn was a single crystal along the <220> direction. The cluster was synthesized by square wave electrodeposition. By changing the deposition factors, a mixture of thorns and particles was synthesized, where each thorn grew on one basis and the thorn was composed of dodecahedral bases. Compared with the mixture, the cluster had higher activity toward the electrooxidation of formic acid, and also much higher activity than Pd powder, which was evidenced by the improved current density and onset potential of formic acid oxidation. The fact that pure thorn clusters had a higher catalytic activity than the mixture of thorns and particles proved that the higher activity was ascribed to the single crystal property of the thorns.

1. Introduction

Palladium, as one of the Pt-group metals, has been applied in electrochemistry,[1,2] nano-scale electronic devices,[3] automobile pollutant reduction[4] and so on. Palladium is normally used as pure Pd powders or is carbon supported, where Pd appears in the form of nano-sized particles.[5] The shape control of nanocrystals has become one of the crucial challenges in nano-technology, since the morphology of the nano-material will influence both its physical and chemical properties.[6] For example, tetrahexahedral shaped Pt crystals show an enhanced catalytic activity, up to 400% per unit surface area, compared with Pt particles, which is explained by the high index degree of the tetrahexahedral crystal surface.[7] A novel dendritic Pd nanostructure has been synthesized and used to construct a H_2O_2 sensor. The dendritic structured Pd showed better stability and a wider linear range compared with spherical Pd particles.[8] Xia's group performed a series of studies on nano-structured Pd materials, such as octahedral, decahedral, icosahedral, triangular and hexagonal Pd, Pd nanoboxes, nanocages, nanobars and nanorods.[9–11] Various methods have been employed to obtain different architectures, including template synthesis,[12,13] vapor deposition[14–16] and colloidal synthesis,[17,18] *etc.* The template method is efficient in constraining the growth of the metal into desired geometrical architectures,[19] however, it always needs tedious pre-synthesis and after-removal steps. In spite of the many attempts which have been made to prepare single crystalline palladium without a template,[20–23] few reports appear on the preparation of one-dimensional Pd nanomaterials.

Electrodeposition, as a traditional electrochemical technique, has been proved a useful tool in preparing shape-controlled nanocrystals.[2,7] The diversity of the parameters in electrodeposition brings great variety in architectures. Recently, high index faceted tetrahexahedral platinum nanocrystals,[7] nanotubes[24] and nanowires[25,26] were synthesized by electrodeposition. Compared

[a]*The Key Laboratory of Low-carbon Chemistry & Energy Conservation of Guangdong Province, The State Key Laboratory of Optoelectronic Materials and Technologies, Sun Yat-sen University, Guangzhou, 510275, PR China. E-mail: menghui@mail.sysu.edu.cn; stsspk@mail.sysu.edu.cn; Fax: +86 20 84113369; Tel: +86 20 84036736*
[b]*Materials Physics & Applications Division, Los Alamos National Laboratory, Los Alamos, NM, 87545, USA*

Broader context

Palladium has lots of applications in energy and environment related fields. Conventionally, Pd is always used in the form of Pd black or loaded on carbon. In this work, Palladium thorns were prepared by the electrodeposition method. By controlling the deposition parameters, the products could be accordingly controlled. The thorn could be composed of dodecahedral units and each thorn stood isolated from each other. Another kind of thorn based on hexahedral units formed a thorn cluster. The whole thorn was a single crystal along the <220> direction. The Pd thorns were characterized for the electrochemical oxidation of formic acid and showed good kinetic activity. This material can find applications in energy devices such as direct liquid fuel cells and in other fields where Pd is used.

with other methods, electrodeposition has the advantages of being simple, convenient, free of templates and effective for shape control.

A fuel cell is an environmentally friendly electrochemical power supply, and fuel cells fuelled by liquid fuels such as alcohol or formic acid have the biggest possibility of being commercialized for portable use. Palladium works as the best anode electrocatalyst in a direct formic acid fuel cell.[27–30] Palladium is also a highly efficient electrocatalyst for ethanol electrooxidation in an alkaline environment. Shen's group[31–34] performed a series of studies on Pd electrocatalysts and some unusual phenomena on the electrooxidation of ethanol were found. Although Pd particles are highly active in alkaline environments, higher Faradic efficiency is expected on novel architectures.

Here, we report the preparation of pure Pd thorn clusters which are composed of one-dimensional single crystalline Pd nanothorns (Pd/NT) by the potential square wave electrodeposition method. The Pd thorns were manipulated using the deposition potential and gathered into clusters. By controlling the electrodeposition parameters, pure Pd thorn clusters were deposited on the surface of the electrode without particles. In the electrooxidation of formic acid, the pure Pd thorn clusters showed better performance than the mixture of Pd thorns and particles, proving the higher catalytic activity of Pd thorns.

2. Experimental

All chemicals were of analytical grade and used as received.

2.1 Preparation of the Pd/NT

Pd/NT was deposited on the surface of a graphite rod with a diameter of 0.6 cm from Poco Graphite, Inc. The top surface of the rod was polished using a succession of sandpapers and a polishing cloth on a polishing machine, then, finally, ultrasonically cleaned. The cylindrical surface of the graphite rod was painted with an insulating varnish, leaving the polished surface as a working electrode. Pd/NT was synthesised by a two-step potential square wave electrodeposition in a solution of 2 mM K_2PdCl_6 in 0.5 M H_2SO_4 on a Bio-Logic VMP3 potentiostat. Briefly, the square wave electrodeposition held the potential at a certain E_1 value for a certain T_1 time, then switched to another potential E_2 and T_2 time to finish one cycle. The cycle was repeated for specified times. In this work, a kind of two-step square wave method was applied. The first step was the nuclei growing step and the second was the crystal growing step. For the preparation of a Pd thorn cluster, in the first step E_1, T_1, E_2 and T_2 were 0.8 V, 0.05 s, 0.2 V and 0.02 s, respectively. The number of the square wave was 600. For the second step E_1, T_1, E_2 and T_2 were 0.6 V, 0.005 s, 0.25 V and 0.005 s, respectively. The number of the square wave was 18 000. For the preparation of the mixture of Pd thorns and particles, E_2 was set at −0.1 V with all other parameters remaining the same as for the Pd thorn clusters in the first step.

2.2 Physical characterization of the Pd/NT

The morphology and structure of the hierarchical nanostructures were characterized by thermal field emission environmental scanning electron microscopy (Quanta 400, operating at 15 kV), and by transmission electron microscopy (TEM, JEOL JEM-2010HR, operating at 200 kV). The as-prepared samples were observed with SEM without any treatment. For TEM observations, the surface layer of the graphite rod was scraped to get powder, mixed with ethanol, and treated in an ultrasonic bath. Finally, a drop of the suspension was transferred to a carbon film-coated copper grid, followed by solvent evaporation under ambient conditions. X-ray photoelectron spectroscopy was used to determine the chemical bonding state and surface composition of the Pd/NT. The XPS spectra were acquired using an ESCA Lab 250 (Thermo VG) with 200 W Al Kα radiation in a twin anode and the distance between the X-ray gun and sample was about 1 cm. The analysis chamber pressure was about 2×10^{-7} Pa and the pass energy was 20 eV for high resolution scans. The surface of the sample was cleaned with Ar before testing.

2.3 Electrochemical characterization of the Pd/NT

The electrooxidation of formic acid on the Pd thorn clusters and the mixture of Pd thorn particles was tested in a solution of 0.2 M formic acid/0.1 M H_2SO_4 by cyclic voltammetry in a standard three-electrode cell at room temperature. A Pt foil served as the counter electrode, with a saturated calomel electrode (SCE) as the reference electrode. Cyclic voltammetry measurements were carried out on a Bio-Logic VMP3 potentiostat with a sweep rate of 50 mV s^{-1}. All current data shown in this work are normalized by electrochemical active surface area.

3. Results and discussion

A two-step potential square wave electrodeposition method was used to synthesize the Pd/NT.[2] The first step was the formation of nuclei and the second was the electro-growth of metal crystals on the nuclei.[2,7] Considering the reduction potential of Pd^{4+} in $PdCl_6^{2-}$, the nuclei formation potential was chosen as 0.8 V (*vs.* SCE); the wave was varied by the lower potential values, which were 0 to −1 V (*vs.* SCE). It turned out that the length and accumulation state of the product were determined by the potentials applied in the nuclei formation step. This method succeeded in the formation of Pd/NT that were grown on a dodecahedron basis. However, there were particles of irregular shape mixed in with the NTs. In this work, pure Pd thorn clusters were synthesized by optimizing the deposition parameters. Fig. 1 compares the morphologies of the Pd thorn cluster and the Pd thorn/particle mixture. Fig. 1a shows a uniform dispersion of Pd thorn clusters covering the surface of the electrode. From an enlarged picture (Fig. 2a), it is clear that the surface of the electrode was covered by pure Pd thorn clusters without particles. Figs 1c and 1d were synthesized at the nuclei potential of 0.8 V to −0.1 V (*vs.* SCE), and the results are similar to those reported.[2] The surface of the electrode was covered by a mixture of particles and Pd/NT. The particles might be of different special shapes, but the shape could not be controlled. The Pd nanothorns grew on a dodecahedron basis and only one nanothorn was formed on one nuclei basis. The length of the nanothorns could be controlled from 100–700 nm, with diameters from 30–70 nm. The diameter of the particles was 20–50 nm. Various methods had been tried to get pure Pd/NT. In this work, the nuclei potential was set as 0.8–0.2 V, followed by the same crystal

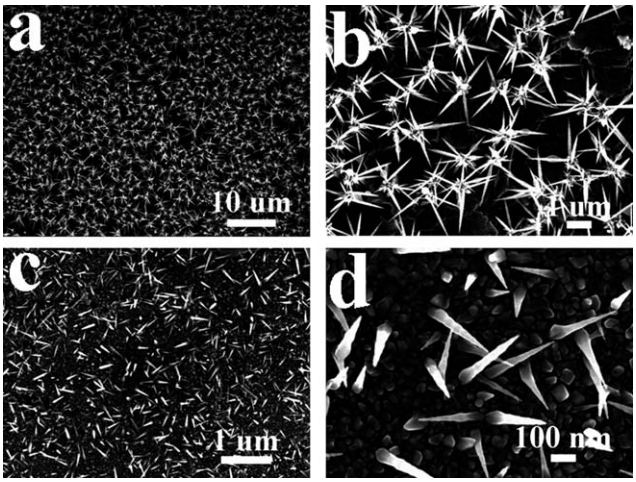

Fig. 1 SEM micrographs of pure Pd thorn clusters (a, b) and the mixture of Pd thorns and Pd particles (c, d).

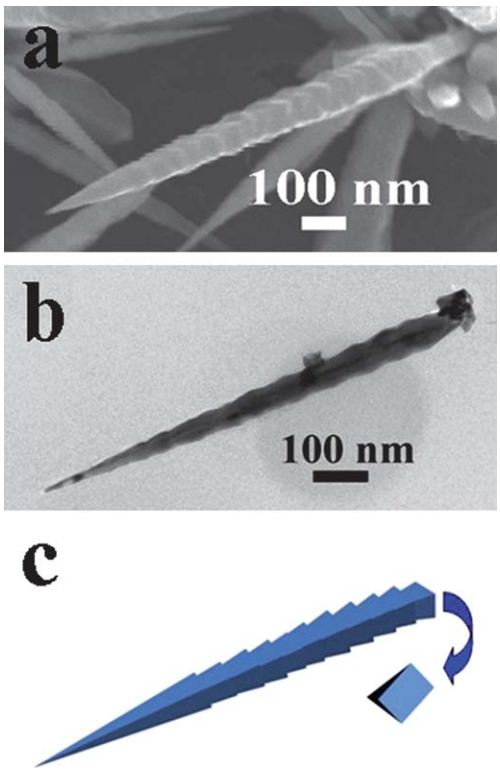

Fig. 2 SEM (a), TEM (b) micrograms and proposed structure (c) of a single thorn in the thorn cluster.

growth step which is 0.6–0.2 V. The products were pure Pd thorn clusters without particles.

Fig. 2 shows the SEM and TEM images of a selected single thorn from the cluster. SEM and TEM gave the same information about the thorn. The thorn was composed of segments built up on each other with their diameter reducing gradually to form the tip. This was different to what was reported for the thorn/particle mixture, where the thorn grew on a dodecahedral basis, the thorn of the cluster was based on a hexahedral basis. This was evidenced by Fig. 3. The cross-section of a broken thorn showed

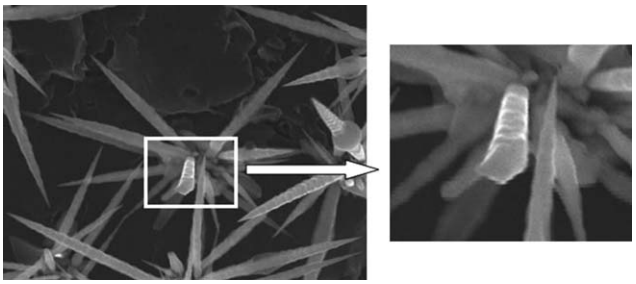

Fig. 3 SEM micrograms of a Pd cluster with a broken thorn and an enlarged cross-section of the thorn.

a quadrilateral surface, which proved that the segment was hexahedral. For a dodecahedron, the cross-section was a pentagon. Based on the information from Fig. 2a and b and the cross-section in Fig. 3, a schematic diagram of the structure of the thorn was prepared, as shown in Fig. 2c. The thorn was composed of hexahedrons of decreasing size.

The results showed that by varying the deposition parameters, especially in the nuclei growth step, the morphology of the product could be controlled. The product might be the mixture of thorns and particles, where the thorn grew on a dodecahedral basis. The pure thorn clusters without particles, which were synthesized under optimized conditions, grew on a hexahedral basis. Fig. 4 shows a schematic diagram of the evolution of the thorns. According to the solution–liquid–solution (SLS) growth process, the growth of the thorn crystal was divided into two steps: nucleation and crystal growth. In the nucleation step (Fig. 4a), a small nucleus was reduced from the solution. This was an electroreduction step, during which the following reaction took place:

$$PdCl_6^{2-} + 2e^- \rightarrow PdCl_4^{2-} + 2Cl^- \quad E^o = 1.05\ V\ (SCE) \qquad (1)$$

$$PdCl_4^{2-} + 2e^- \rightarrow Pd + 4Cl^- \quad E^o = 0.382\ V\ (SCE) \qquad (2)$$

The reduction potential was 0.8 V (SCE), held for 50 ms. A lower potential was used to form a square wave pulse. The values of the lower potential were chosen from 0 to −1 V (SCE). The results proved that these parameters were successful for the formation of Pd thorns, and the value of the lower potential had a big influence on the morphology of the product. The reduction step (1) could take place at a potential of 0.8 V. At a lower potential, $PdCl_6^{2-}$ was absorbed on the defects of the electrode surface. If the lower potential was set at 0.2 V, the reduction step (2) also took place. When the absorbing potential was set

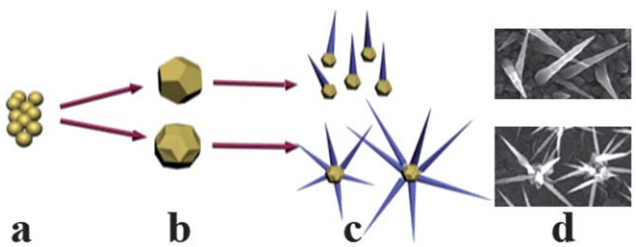

Fig. 4 A schematic diagram of the growth mechanism of Pd thorns with different nuclei.

between 0 and −1 V, at each reduction step Pd nuclei were formed on the surface of the electrode, part of which reduced into particles. This was why with such parameters the product was a mixture of Pd thorn and particles. When the lower potential was chosen as 0.2 V, the potential was not favourable for the absorption of $PdCl_6^{2-}$ on the electrode surface, but favourable for the reduction of $PdCl_4^{2-}$. Because of the preference of $PdCl_6^{2-}$ adsorption on the newly formed Pd atom, palladium nuclei continue to grow into crystals and no particles were formed. Fig. 4b shows two proposed nuclei. As reported, when the product was a mixture of thorns and particles, the thorns were based on a dodecahedron and composed of a series of dodecahedra of decreasing size. Only one thorn grew from one dodecahedral nucleus, as shown in Fig. 4c and 4d (upper images). When the lower potential was set at 0.2 V, the thorn was based on a hexahedral basis, as shown in Fig. 2c and Fig. 3. Based on the fact that more than one thorn grew on one nucleus and the cross-section of the thorn was quadrilateral, the nucleus was proposed to be multifaceted with each facet to be quadrilateral as shown in Fig. 4b. More than one thorn grew, in different directions based on the nucleus, resulting in the clusters as shown in Fig. 4c and 4d (lower images).

X-ray photoelectron spectroscopy (XPS) was used to study the metallic character of the Pd/NT. The Pd3d narrow scan spectrum of the NT is shown in Fig. 5. The surface of the nano metallic material was covered by a layer of metal oxide because of the exposure of the material to air. Before XPS testing, the sample was cleaned at a rate of 2 nm min^{-1} in a vacuum chamber for 5 min, leaving only the inner surface to be subjected to X-ray irradiation. As displayed in Fig. 5, the spectra showed only two asymmetric Pd peaks, assigned to $Pd_{5/2}$ and $Pd_{3/2}$, with binding energies of 335.3 and 340.6 eV, revealing results typical of Pd metal for both the mixture of Pd/NT/particles and pure Pd thorn clusters.[35] The consistency of the XPS results for both products proved the feasibility of producing Pd metal by the electrodeposition method.

The TEM image in Fig. 2b, along with the SEM results, proved the thorn structure of the product. The crystalline structure information for the thorn was obtained by HRTEM as shown in Fig. 6. Fig. 6a is the HRTEM image of a segment of the thorn, and Fig. 6b is the HRTEM image of the tip of the thorn. Fig. 6a shows well resolved continuous fringes with the same orientation. These fringes could be observed from the basis to the tip of the thorn. The main fringes lying parallel to the thorn are the (111) facet, with fringe spacing of 0.23 nm, which is typical for face-centered cubic (fcc) Pd crystals. The crystal growth

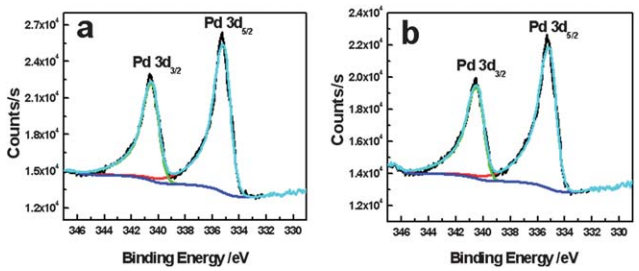

Fig. 5 XPS spectra of a pure Pd thorn cluster (a) and a mixture of Pd/NT/particles (b).

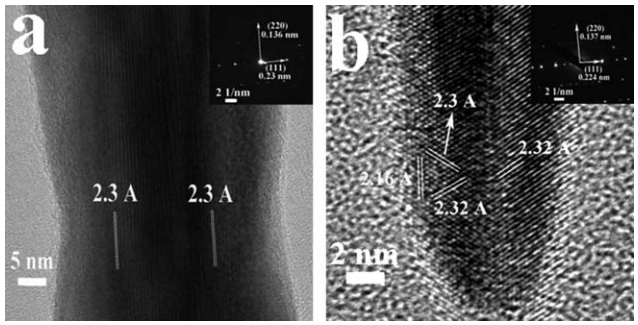

Fig. 6 HRTEM micrographs of the body (a) and tip (b) of a Pd thorn and corresponding selected area electron diffraction (SAED) diagrams (insets).

orientation was the <220> direction, which was perpendicular to the (111) facet. From the selected area electron diffraction (SAED) of Fig. 6a, two sets of spots could be identified, which were (111) and (220), with d-spacings of 0.23 and 0.136 nm, respectively. These results indicate that the main axis of the thorn is along the (111) facet and the growth of the thorn occurred along the (220) facet, which was perpendicular to the (111) facet. The diameter of the tip was about 2 nm. As proposed in Fig. 2, the tip should have four facets. Due to the orientation of the electron beam of the TEM, only two facets could be observed in Fig. 6b. The tip also shows the typical (111) facet fringes, which is in accordance with the body of the thorn. The SAED inset in Fig. 6b also shows two sets of spots, corresponding to the (111) and (220) facets of the fcc crystal. The HRTEM and SAED results show detailed structural information for the Pd thorns, revealing that the whole thorn is a single crystal growing along the <220> direction.

Palladium is a promising electrocatalyst for the electro-oxidation of formic acid. Unlike on Pt, on a Pd electrocatalyst formic acid is oxidized to CO_2 without producing the poisoning intermediate CO. Most studies used Pd powder or Pd particles loaded on carbon supports as electrocatalysts for the oxidation of formic acid. The mixture of Pd thorns and particles showed better performance for formic acid oxidation in terms of the peak potential and peak current density.[2] Pure Pd thorn clusters were

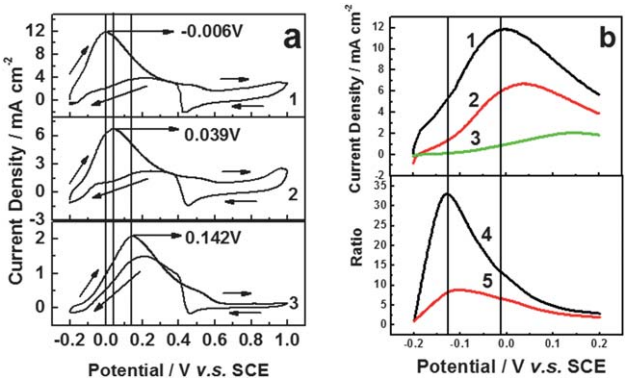

Fig. 7 (a) Cyclic voltammograms of the electrooxidation of formic acid on pure Pd thorn clusters (1), a mixture of thorns and particles (2), and Pd powder (3) in 0.1 M H_2SO_4/0.2 M formic acid at a sweep rate of 50 mV s^{-1}. (b) Current densities of 1–3, and current ratios of 1 to 3 (4) and 2 to 3 (5).

synthesized in this work and the electroactivity for formic acid oxidation is shown in Fig. 7a1. Fig. 7a2 shows the cyclic voltammogram (CV) of formic acid oxidation on the mixture of Pd thorns and particles. Compared with the mixture, the peak potential of formic acid oxidation on pure Pd thorns showed a slight shift towards the negative direction and the peak current density almost doubled that of the mixture. This proved that the pure Pd thorn clusters had higher electroactivity than the mixture of thorns and particles. In comparison with the performance of the Pd powder, as shown in Fig. 7a3, the peak potential of the CV of the mixture shifted negatively by 100 mV and the peak current density increase was three times greater. For the pure Pd thorns, the increase in the current density was almost six times that of the Pd powder. These results evidenced the improvement in the catalytic activity of the single crystal of Pd due to the much more preferential crystalline facets. The activity for formic acid oxidation on the mixture is higher than on the Pd powder. The Pd thorns grew along the <220> direction and the crystalline surface along the (111) facet is the best for liquid fuel electrooxidation. Fig. 7b shows the current ratios for formic acid oxidation on Pd black compared to pure Pd/NT or mixed Pd/NT and particles. It is clear that the currents are much higher at interesting potentials, showing the improvement in the kinetics.

4. Conclusions

By controlling the electrodeposition parameters, especially the potentials in the nuclei forming step, Pd materials with different morphologies were synthesized. With the nuclei potential of (0.8 V, 0.2 V), the thorn grew on a hexahedral basis and several thorns grew from one nucleus forming a thorn cluster. No particles were formed in this situation. With the nuclei potential of (0.8 V, −0.1 V), the thorns grew on dodecahedral bases, and only one thorn grew on one nucleus. Besides the thorns, there were also particles present in the product. The HRTEM results proved that the thorns in both situations had the same growth direction of <220>, and the whole thorn was one single crystal. The thorn clusters were proved to have higher electroactivity for the electrooxidation of formic acid compared with the mixture of thorns and particles.

Acknowledgements

The work was supported by the National Natural Science Foundation of China (21073241, U1034003) and the China National 863 Program (2009AA034400) and the Foundation of the State Key Laboratory of Optoelectronic Materials and Technologies (2010-ZY-4-7). Dr H. Meng thanks the New Teacher Funding of Sun Yat-sen University (30000-3126170), Strategic Cooperation Project between Guangdong Province and Chinese Academy of Sciences (2010-30000-4202493) and Doctoral Fund of Ministry of Education of China (20100171120022).

References

1 S. E. Habas, H. Lee, V. Radmilovic, G. A. Somorjai and P. D. Yang, *Nat. Mater.*, 2007, **6**, 692–697.
2 H. Meng, S. Sun, J. P. Masse and J. P. Dodelet, *Chem. Mater.*, 2008, **20**, 6998–7002.
3 A. Javey, J. Guo, Q. Wang, M. Lundstrom and H. Dai, *Nature*, 2003, **424**, 654–657.
4 Y. Nishihata, J. Mizuki, T. Akao, H. Tanaka, M. Uenishi, M. Kimura, T. Okamoto and N. Hamada, *Nature*, 2002, **418**, 164–167.
5 H. Li, G. Sun, Q. Jiang, M. Zhu, S. Sun and Q. Xin, *Electrochem. Commun.*, 2007, **9**, 1410–1415.
6 Y. N. Xia, P. D. Yang, Y. G. Sun, Y. Y. Wu, B. Mayers, B. Gates, Y. D. Yin, F. Kim and H. Q. Yan, *Adv. Mater.*, 2003, **15**, 353–389.
7 N. Tian, Z. Y. Zhou, S. G. Sun, Y. Ding and Z. L. Wang, *Science*, 2007, **316**, 732–735.
8 P. Zhou, Z. H. Dai, M. Fang, X. H. Huang and J. C. Bao, *J. Phys. Chem. C*, 2007, **111**, 12609–12616.
9 B. Lim, Y. J. Xiong and Y. N. Xia, *Angew. Chem., Int. Ed.*, 2007, **46**, 9279–9282.
10 Y. J. Xiong and Y. N. Xia, *Adv. Mater.*, 2007, **19**, 3385–3391.
11 Y. J. Xiong, J. M. Mclellan, Y. D. Yin and Y. N. Xia, *Angew. Chem., Int. Ed.*, 2007, **46**, 790–794.
12 R. A. Pai, R. Humayun, M. T. Schulberg, A. Sengupt, J. N. Sun and J. J. Watkins, *Science*, 2004, **303**, 507–510.
13 T. Thurn-Albrecht, J. Schotter, G. A. Kästle, N. Emley, T. Shibauchi, L. Krusin-Elbaum, K. Guarini, C. T. Black, M. T. Tuominen and T. P. Russell, *Science*, 2000, **290**, 2126–2129.
14 D. Hausmann, J. Becker, S. L. Wang and R. G. Gordon, *Science*, 2002, **298**, 402–406.
15 Y. L. Li, I. A. Kinloch and A. H. Windle, *Science*, 2004, **304**, 276–278.
16 M. S. Gudiksen, L. J. Lauhon, J. F. Wang, D. C. Smith and C. M. Lieber, *Nature*, 2002, **415**, 617–620.
17 E. V. Shevchenko, D. V. Talapin, A. L. Rogach, A. Kornowski, M. Haase and H. Weller, *J. Am. Chem. Soc.*, 2002, **124**, 13958–13958.
18 Y. Sun and Y. Xia, *Science*, 2002, **298**, 2176–2179.
19 C. W. Xu, H. Wang, P. K. Shen and S. P. Jiang, *Adv. Mater.*, 2007, **19**, 4256–4259.
20 Y. Xiong, J. M. McLellan, J. Chen, Y. Yin, Z. Y. Li and Y. Xia, *J. Am. Chem. Soc.*, 2005, **127**, 17118–17127.
21 Y. Xiong, H. Cai, B. J. Wiley, J. Wang, M. J. Kim and Y. Xia, *J. Am. Chem. Soc.*, 2007, **129**, 3665–3675.
22 Y. Xiong and Y. Xia, *Adv. Mater.*, 2007, **19**, 3385–3391.
23 P. Zhou, Z. Dai, M. Fang, X. Huang and J. Bao, *J. Phys. Chem. C*, 2007, **111**, 12609–12616.
24 M. S. Sander and H. Gao, *J. Am. Chem. Soc.*, 2005, **127**, 12158–12159.
25 Z. L. Xiao, C. Y. Han, W. K. Kwok, H. H. Wang, U. Welp, J. Wang and G. W. Crabtree, *J. Am. Chem. Soc.*, 2004, **126**, 2316–2317.
26 F. Favier, E. C. Walter, M. P. Zach, T. Benter and R. M. Penner, *Science*, 2001, **293**, 2227–2231.
27 N. Hoshi, K. Kida, M. Nakamura, M. Nakada and K. Osada, *J. Phys. Chem. B*, 2006, **110**, 12480–12484.
28 W. P. Zhou, A. Lewera, R. Larsen, R. I. Masel, P. S. Bagus and A. Wieckowski, *J. Phys. Chem. B*, 2006, **110**, 13393–13398.
29 D. Bera, S. C. Kuiry and S. Seal, *J. Phys. Chem. B*, 2004, **108**, 556–562.
30 W. Zhou and J. Y. Lee, *Electrochem. Commun.*, 2007, **9**, 1725–1729.
31 C. Bianchini and P. K. Shen, *Chem. Rev.*, 2009, **109**, 4183–4206.
32 P. K. Shen and C. Xu, *Electrochem. Commun.*, 2006, **8**, 184–188.
33 Z. Y. Wang, F. P. Hu and P. K. Shen, *Electrochem. Commun.*, 2006, **8**, 1764–1768.
34 F. P. Hu, P. K. Shen, Y. L. Li, J. Y. Liang, J. Wu, Q. L. Bao, C. M. Li and Z. D. Wei, *Fuel Cells*, 2008, **8**, 429–435.
35 T. Thurn-Albrecht, J. Schotter, G. A. Kästle, N. Emley, T. Shibauchi, L. Krusin-Elbaum, K. Guarini, C. T. Black, M. T. Tuominen and T. P. Russell, *Science*, 2000, **290**, 2126–2129.

